Kruchinin N.Yu. *Nanosystems: Phys. Chem. Math.*, 2025, **16** (5), 650–659. http://nanojournal.ifmo.ru **DOI 10.17586/2220-8054-2025-16-5-650-659**

Controlled release of homogeneous polypeptides from carbon nanotubes with varying PH: molecular dynamics simulation

Nikita Yu. Kruchinin^{1,a}

¹Orenburg State University, Center of Laser and Informational Biophysics, Orenburg, Russia

^akruchinin_56@mail.ru

Corresponding author: N. Yu. Kruchinin, kruchinin_56@mail.ru

PACS PACS 36.20.-r, 02.70.Ns, 61.46.+w

ABSTRACT Using molecular dynamics simulation at different pH levels, changes in the conformations of homogeneous polypeptides located singly or in pairs inside a carbon nanotube were studied. The radial distributions of the density of polypeptide atoms, the distribution of macrochain atoms along the nanotube axis, and the dependences of various components of the potential energy of the nanosystem were calculated. At the isoelectric point, the polypeptides were located in the central part of the carbon nanotube, spreading out along its walls. As the pH level deviated from the isoelectric point, the polypeptide located singly inside the carbon nanotube first unfolded and stretched along its axis, and when almost all links of the macromolecule acquired an electric charge, it exited the nanotube. Polypeptides located in pairs inside the carbon nanotube repelled each other with a change in the pH value and shifted to opposite ends of the nanotube, being released from it.

KEYWORDS molecular dynamics, carbon nanotube, polypeptide, pH, conformation, controlled release.

ACKNOWLEDGEMENTS The study was carried out with the financial support of the Ministry of Science and Higher Education of the Russian Federation within the framework of a grant for conducting large scientific projects in priority areas of scientific and technological development 075-15-2024-550.

FOR CITATION Kruchinin N.Yu. Controlled release of homogeneous polypeptides from carbon nanotubes with varying PH: molecular dynamics simulation. *Nanosystems: Phys. Chem. Math.*, 2025, **16** (5), 650–659.

1. Introduction

Currently, hybrid nanosystems consisting of carbon nanotubes with polymer macromolecules are widely used in the creation of various electrochemical and optical biosensors [1–7], as well as nanocarriers for drug delivery [8–10]. Flexible and uncharged peptide and lipid molecules are adsorbed on the outer surface of the carbon nanotube and form a polymer shell [11,12]. Highly charged and rigid macromolecules of polyelectrolytes, such as DNA [13] or synthetic polymers [14], wrap around the carbon nanotube. A similar nature of conformational changes in polypeptides was observed in molecular dynamics simulation on the surface of metal nanoparticles of various shapes (spherical, cylindrical and spheroidal) [15–18].

A different picture will be observed when polymer molecules are located inside a single-walled carbon nanotube. A number of studies have investigated the encapsulation of peptides inside a carbon nanotube, the transport of peptides under the influence of an external electric field inside a carbon nanotube and the pulling of short peptides through it, as well as the release of protein and peptide molecules encapsulated in a carbon nanotube under the influence of an external electric field [19–28]. In papers [20, 21], it was shown that a peptide molecule is encapsulated inside a carbon nanotube and oscillates near the center of the nanotube, where the Van der Waals interaction energy between the peptide and the carbon nanotube is minimal. It was shown that carbon nanotubes are capable of capturing peptide and protein molecules, with shorter nanotubes capable of encapsulating a peptide with a lower potential well depth [20, 21].

When the pH level changes, the conformations of peptides change significantly [29–31]. This is due to the fact that the more the value of the hydrogen index differs from the value of the isoelectric point of the peptide, the greater the charge acquired by the macromolecule, which becomes polyelectrolyte. In this case, the rigidity of the macrochain increases increasingly due to the repulsion of the polypeptide links from each other. Therefore, if the polypeptide is inside a carbon nanotube, then when the hydrogen index of the environment changes, its conformational structure should also change. And this can lead to the release (decapsulation) of the macromolecule located inside the carbon nanotube. Small medicinal or photoactive molecules can be associated with the polypeptide located inside the carbon nanotube. When the pH of the medium changes and, accordingly, the conformational structure of the polypeptide undergoes a significant restructuring, small molecules can be decapsulated from the nanotube separately or together with the macrochain. This effect can be used to create a nanocontainer with a controlled release of drugs or photoactive label molecules when the pH of the medium changes.

Of great interest is also the restructuring of the conformations of several polypeptide molecules located inside the carbon nanotube when the pH level changes. If the molecules of homogeneous polypeptides have the same composition of amino acid residues, then when the pH value deviates from the isoelectric point, they are charged with the same charge sign. This leads to the repulsion of like-charged polypeptides from each other and to a significant change in their configuration inside the carbon nanotube, which can lead to the expulsion of macromolecules from the carbon nanotube.

Thus, the aim of this work is to study changes in the conformational structure of macromolecules of homogeneous polypeptides located inside a single-layer carbon nanotube, singly and in pairs, when changing pH.

2. Molecular dynamics simulation

Full-atom molecular dynamics (MD) simulations were performed using the NAMD 2.14 software package [32] for a molecular system in which one or two identical polypeptide molecules were located inside a carbon nanotube. A single-walled carbon nanotube with a length of 30 nm, a diameter of about 6 nm, and a chirality of n = 45 and m = 45 was considered. The atoms of the nanotube remained fixed during the simulation.

The choice of a carbon nanotube of such a diameter was due to the need to place a polypeptide macromolecule in a coil conformation in the starting configuration, which had a sufficiently large size, inside it. In works [20–22], the processes of encapsulation of shorter peptides in a carbon nanotube of different diameters (from 2.2 to 3.8 nm) were considered, and with equal chirality indices n=m. Therefore, in this work, a carbon nanotube with the same chirality indices was also considered. In general, for nanotubes of the same diameter, but with different chirality indices, the results should not change significantly, since the main contribution to the encapsulation of peptides and their adsorption inside a carbon nanotube is made by the Van der Waals interaction of the peptide with the walls of the nanotube. Since the number of atoms for nanotubes of similar diameter, but with different chirality will be almost the same, then in general the interaction of the peptide with the walls of the carbon nanotube will be the same, and therefore the decapsulation of the macrochain will occur under the same conditions.

The pH level was changed indirectly, as was done in [29]. MD simulation was performed for polypeptides consisting of 100 amino acid residues of glutamic acid at different pH values. In the range of pH \approx 6–8, corresponding to a neutral medium, all amino acid residues of glutamic acid Glu have a negative charge of -1e according to the titration curve. When the increasing of the acidity of the medium and the decreasing of the pH value begins, the proportion of amino acid residues in the polypeptide changes. It leads to changing their charge and becoming neutral Glu⁰ [29]. Upon reaching the isoelectric point pI=3.22, all amino acid residues of glutamic acid in the macrochain become uncharged Glu⁰.

In this work, a series of polypeptides from glutamic acid units with different proportions of neutral and negatively charged amino acid residues were considered, which corresponded to the state of the polyglutamate macrochain at pH values in the range from the isoelectric point pI=3.22 to a neutral environment pH \approx 6-8:

- 1) Glu₁₀₀ polypeptide (total charge of the macrochain -100e) which corresponds to the values of pH \approx 6–8 according to the titration curve;
 - 2) polypeptide ($Glu_{10}Glu^{0}Glu_{9}$)₅ (total charge -95e) which corresponds to the value of pH \approx 5.8;
 - 3) polypeptide ($Glu_5Glu^0Glu_4$)₁₀ (total charge -90e), pH \approx 5.5;
 - 4) polypeptide ($Glu_2Glu^0Glu_2$)₂₀ (total charge -80e), pH \approx 5;
 - 5) polypeptide (GluGlu⁰Glu)₃₃Glu (total charge -67e), pH \approx 4.6;
 - 6) polypeptide (GluGlu⁰)₅₀ (total charge -50e), pH \approx 4.3;
 - 7) polypeptide ($Glu^0GluGlu^0$)₃₃ Glu^0 (total charge -33e), pH \approx 4;
 - 8) polypeptide $(Glu_2^0GluGlu_2^0)_{20}$ (total charge -20e), pH \approx 3.8;
 - 9) polypeptide ($Glu_5^0GluGlu_4^0$)₁₀ (total charge -10e), pH \approx 3.6;
 - 10) polypeptide ($Glu_{10}^0GluGlu_9^0$)₅ (total charge -5e), pH \approx 3.4;
 - 11) polypeptide Glu_{100}^0 (uncharged macromolecule) at the isoelectric point pI=3.22.

For charged amino acid residues of glutamic acid, the CHARMM36 force field was used [33, 34], and to describe amino acid residues of glutamic acid in the neutral form, the interaction potentials developed in [35] and expanding the CHARMM36 force field were used. The parameters for the carbon atoms of the nanotube were set to the same as for the CA type atoms of the CHARMM36 force field, which are used to describe benzene molecules [36]. The van der Waals potential was cut off at a distance of 1.2 nm using a smoothing function between 1.0 and 1.2 nm. Electrostatic interactions were calculated directly at a distance of 1.2 nm, for larger distances the particle-mesh Ewald (PME) method [37] with a grid step of 0.11 nm was used. The entire molecular system was placed in a parallelepiped with edge dimensions of $54 \times 18 \times 18$ nm, filled with TIP3P water molecules [38]. In total, more than 560 thousand water molecules were placed in the simulation area. Water molecules were also located inside the carbon nanotube. The interaction of water molecules with the polypeptide was also described using the CHARMM36 force field, including electrostatic interactions between partial charges of water molecules and the polypeptide, as well as Van der Waals interactions between atoms of water molecules and the polypeptide via the Lennard-Jones potential. The MD simulation was performed at a constant temperature of 300 K (NVT, Berendsen thermostat). The length of the time trajectory reached 30 ns, the simulation step was 1 fs.

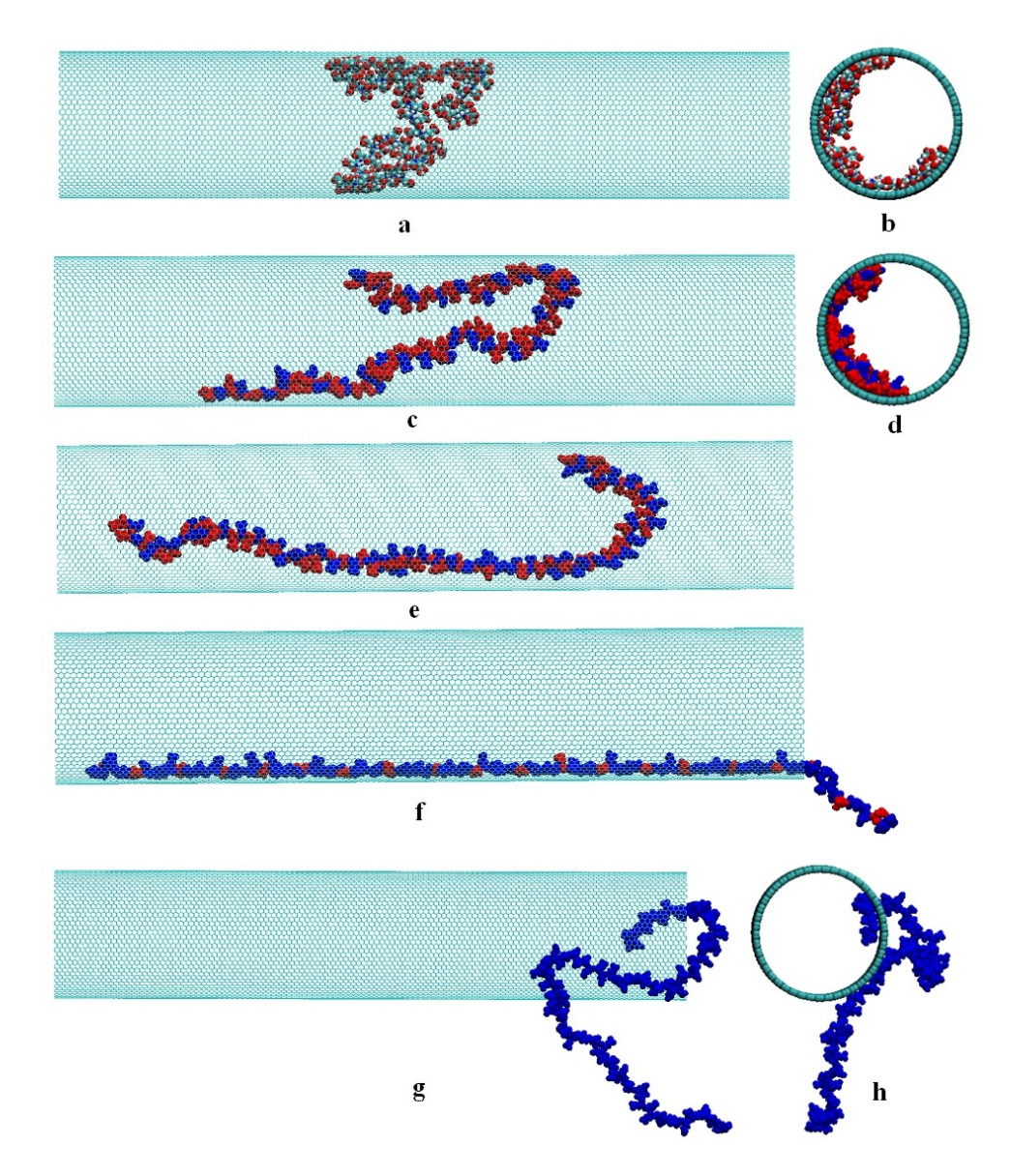


FIG. 1. A single polypeptide of 100 glutamic acid units inside a carbon nanotube after modeling at the isoelectric point pI=3.22 (a, b, each atom is shown in its own color), pH \approx 4 (c and d), pH \approx 4.3 (e), pH \approx 5 (f), pH \approx 6–8 (g and h). Water molecules are not shown for clarity; in figures c–h, uncharged amino acid residues Glu⁰ are shown in red, and negatively charged Glu are shown in blue (a, c, e, f, g – side view, b, d and h – end view)

First, we considered the case when one or two macromolecules of the Glu^0_{100} polypeptide were located inside the carbon nanotube at a pH value equal to the isoelectric point pI=3.22, i.e. when the polypeptides were generally neutral. At the initial moment, the polypeptides were in the form of nonequilibrium coils inside the carbon nanotube. As a result of the modeling, adsorption of both a single macrochain (Fig. 1) and a system of two identical polypeptides (Fig. 5) on the inner surface of the carbon nanotube was observed. The obtained equilibrium structures of the polypeptides at the isoelectric point were subsequently used as starting ones at pH values in the range from 3.22 to 6–8. Three different starting conformations were considered for both a single polypeptide and a complex of two identical polypeptides inside the carbon nanotube.

Based on the results of modeling in the case of adsorption of a macrochain on the inner wall of a carbon nanotube, radial distributions of the density of polypeptide atoms, as well as the distribution of macrochain atoms along the nanotube axis were calculated for all the conformations obtained. The dependences of various components of the potential energy of the nanosystem (total, Van der Waals, electrostatic, as well as torsion angles of the polypeptide) were also calculated when changing the conformational structure of the polypeptide inside the carbon nanotube.

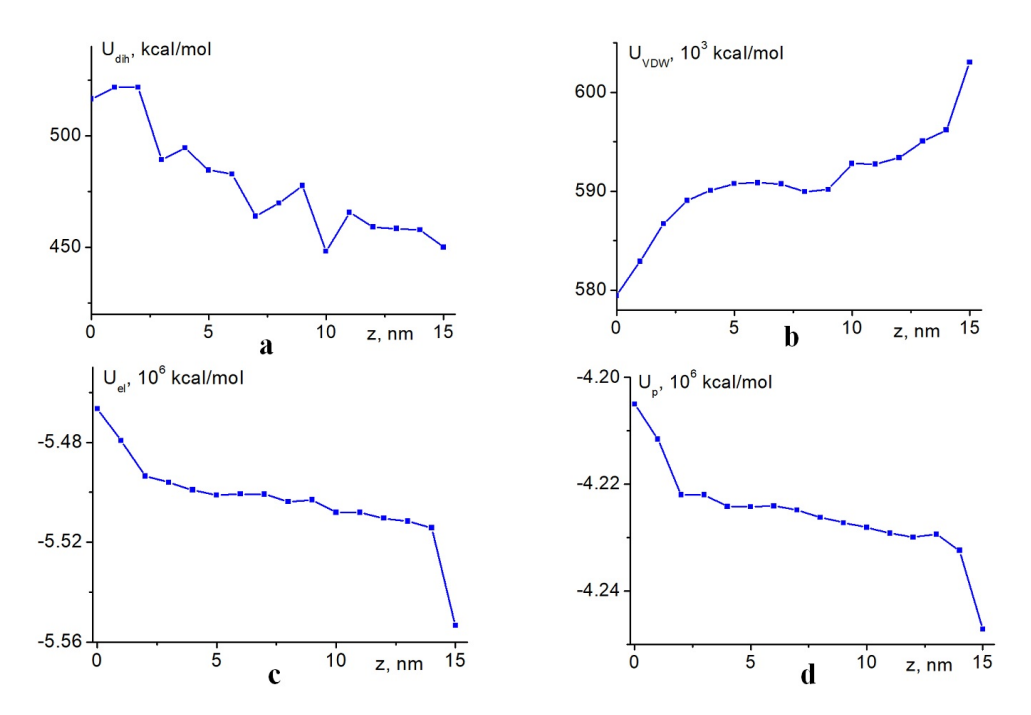


FIG. 2. Dependences of the potential energy of torsion (dihedral) angles (a), van der Waals (b), electrostatic (c) and total potential energy (d) of a single polypeptide inside a carbon nanotube as the center of mass of the macrochain moves away from the center of the nanotube along the axis at pH \approx 6–8

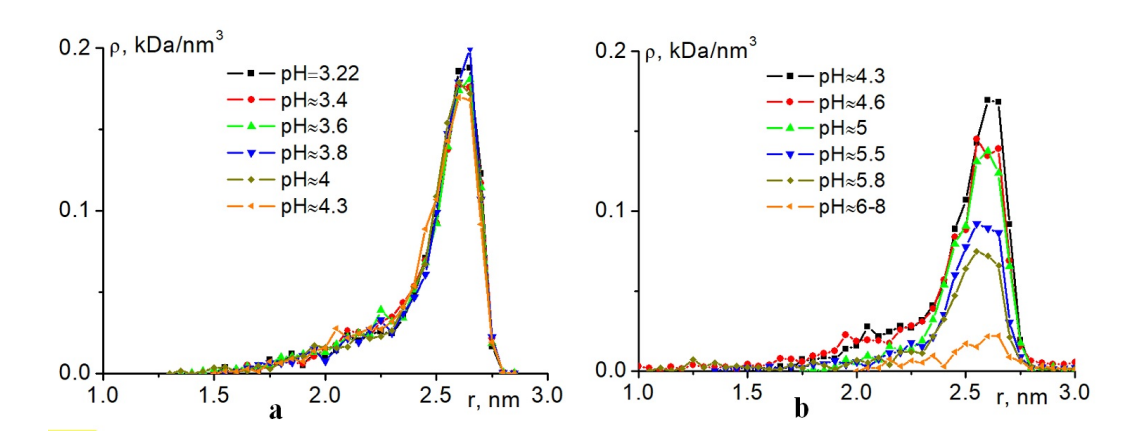


FIG. 3. Radial dependences of the average density of atoms of a single polyglutamate macrochain inside a carbon nanotube at the end of the simulation for different values of pH: a) from 3.22 to 4.3, b) from 4.3 to 6-8

3. Results

3.1. Conformational changes of a single polypeptide macrochain inside a carbon nanotube with pH changes

Figures 1a,b show a single macromolecule of a polypeptide consisting of 100 glutamic acid units after molecular dynamics simulation inside a carbon nanotube at the isoelectric point pI=3.22. In this case, the Glu_{100}^0 macromolecule has a zero electric charge overall and is adsorbed on the inner surface of the nanotube. This is in good agreement with the results obtained in [20–23], where it was shown that the peptide is encapsulated inside a carbon nanotube and this arrangement of the peptide is the most energetically favorable.

As the pH value increased and the isoelectric point deviated, more and more polyglutamate units acquired a negative charge. Therefore, due to the increasingly strong repulsion of the links from each other and, accordingly, the increase in rigidity and persistent length of the macrochain, the polypeptide unfolded more and more (Figs. 1c,d). The macromolecule, initially adsorbed quite compactly on the inner surface of the nanotube (Fig. 1a), began to partially stretch along the nanotube starting from the pH value of pH \approx 4.3 (Fig. 1e), that is, when half of the polypeptide links became negatively charged. Starting with the values of the hydrogen index pH \approx 5, partial decapsulation of the polypeptide from

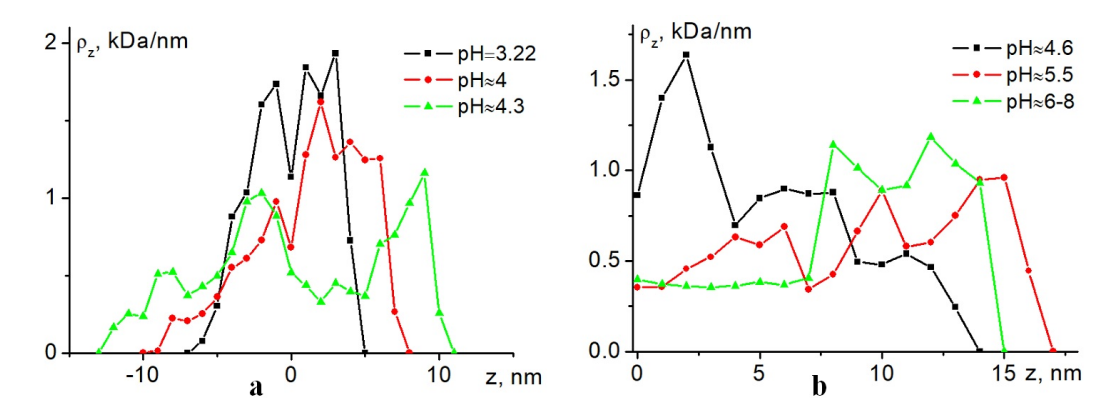


FIG. 4. Distributions of the average linear density of atoms of a single polypeptide from glutamic acid units at the end of the simulation at different values of pH from 3.22 to 4.3 along the axis of the carbon nanotube. b) Distribution of absolute values of the average linear density of atoms of a single polyglutamate with increasing distance from the center (z=0) of the nanotube along the axis of the nanotube at values of pH from 4.6 to 6–8

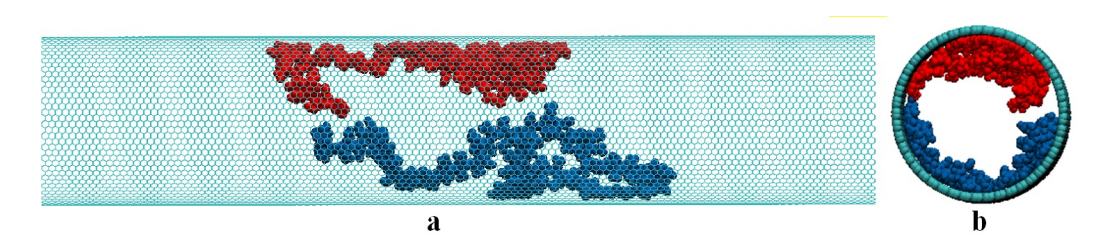


FIG. 5. Two polyglutamate macromolecules after modeling inside a carbon nanotube after MD simulation at pI=3.22 (a – side view, b – end view, the one shown in red and the second one in blue)

the carbon nanotube to the outside began to occur (Fig. 1f). In the case of an increase in the hydrogen index to pH \approx 5.8-8, when all or almost all links of the polypeptide became negatively charged, decapsulation of the polypeptide from the nanotube occurred (Figs. 1g,h). In this case, the polypeptide was concentrated near one of the ends of the carbon nanotube.

Figure 2 shows the dependences of the potential energy of torsion (dihedral) angles, as well as van der Waals, electrostatic and total potential energy of a single polypeptide of 100 glutamic acid units inside a carbon nanotube as the center of mass of the macrochain moves away from the center of the nanotube (z=0) at pH \approx 6-8. The position of the center of mass of the polypeptide at a distance of 15 nm from the center of the nanotube corresponds to the displacement of the macromolecule to the edge of the nanotube (Fig. 1g,h). It can be seen that the potential energy of the torsion angles gradually decreases as the polyelectrolyte unfolds and exits the nanotube (Fig. 2a). In this case, the potential energy of van der Waals interactions during decapsulation of the polypeptide gradually increased (Fig. 2b), which is in good agreement with the dependence of the energy of van der Waals interactions of the peptide with the carbon nanotube presented in [20, 21]. However, in this case, a more significant decrease in the electrostatic energy of the nanosystem occurred (Fig. 2c), which made the greatest contribution to the change in the total potential energy of the nanosystem, which also decreased when the charged polypeptide was shifted to the edge of the carbon nanotube (Fig. 2d). Thus, for the charged macrochain, the conformation in which the polypeptide was located on the outside at the edge of the carbon nanotube turned out to be energetically favorable.

Figure 3 shows a comparison of the radial dependences of the average atomic density of a single polypeptide made of glutamic acid units inside a carbon nanotube at the end of the simulation at different pH values from 3.22 to 4.3 (Fig. 3a) and from 4.3 to 6–8 (Fig. 3b). It is evident that in the range of pH values from 3.22 to 4.3 (Fig. 3a), that is, from the case of a neutral macromolecule to a half-charged one, the density of polypeptide atoms inside the carbon nanotube changed insignificantly, since most of the polypeptide units were adsorbed on its inner surface. In this case, a characteristic maximum of the macrochain atom density is observed near the surface of the nanotube [18], and the radial distribution curve of the average atomic density of the polypeptide drops to zero at approximately half the radius of the carbon nanotube. With an increase in the pH value from 4.3 to 6–8 (Fig. 3b), a significant decrease in the density of polyglutamate atoms inside the carbon nanotube is observed. This is due to the gradual release of the polypeptide from the carbon nanotube as the pH increases (Fig. 1g,h).

Figure 4a shows the distributions of the average linear density of atoms of a single polyglutamate macromolecule along the carbon nanotube axis at the end of the simulation at different values of pH in the range from 3.22 to 4.3. It is evident that at the isoelectric point pI=3.22 the macrochain was concentrated in the center of the carbon nanotube (Fig. 4a,

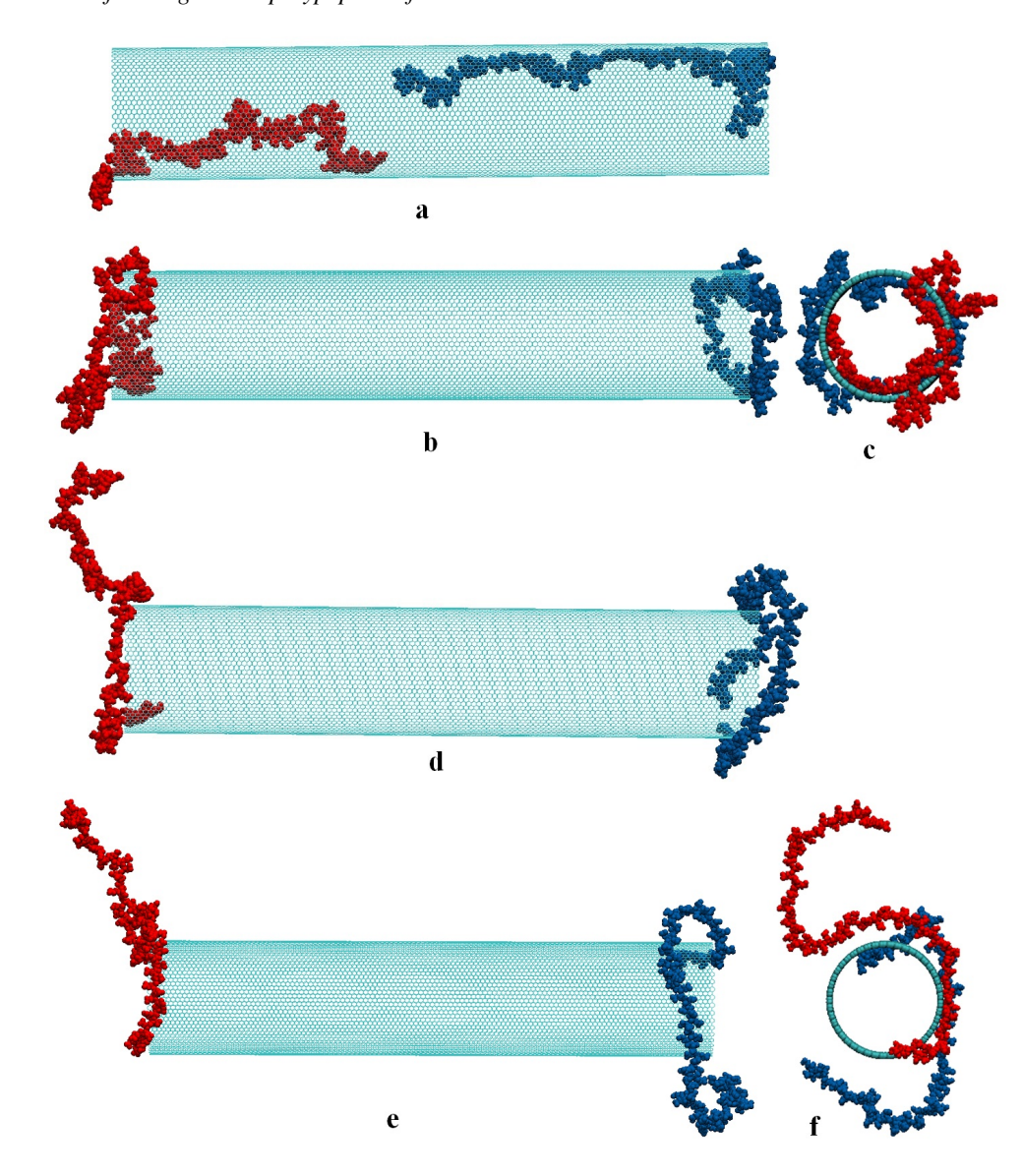


FIG. 6. Two macromolecules of glutamic acid units after modeling inside a carbon nanotube at different pH values: $pH\approx4$ (a), $pH\approx4.3$ (b and c), $pH\approx5$ (d), and $pH\approx6-8$ (e and f). The first polypeptide is shown in red, and the second one in blue (a, b, d, e – side view, c, f – end view)

zero along the z axis). As the hydrogen index increases, the distribution profile of the average density of polypeptide atoms along the nanotube axis broadens due to the increase in the rigidity of the macrochain and its stretching along the nanotube axis

In Fig. 4b, the distributions of absolute values of the average linear density of atoms of a single polyglutamate are shown with increasing distance from the center (z=0) along the nanotube axis at pH from 4.6 to 6–8. It is evident that even at pH \approx 4.6 the macrochain is concentrated mainly in the center of the nanotube, and at pH \approx 5.5 most of the polypeptide links are already shifted to the end of the nanotube, which is associated with the partial exit of the polypeptide to the outside. At pH \approx 6–8 the fully charged macrochain is mostly decapsulated and is located at the end of the carbon nanotube, partially wrapping around it from the outside (Figs. 1g,h).

3.2. Conformational changes of two identical homogeneous polypeptides inside a carbon nanotube with pH changes

A different picture was observed when two identical macromolecules of homogeneous polypeptides were located inside the carbon nanotube. At the initial moment of time at the isoelectric point pI=3.22 they were adsorbed on the inner surface of the carbon nanotube (Fig. 5).

As the pH value increased, the polypeptides gradually became negatively charged, which increased their rigidity and their unfolding inside the carbon nanotube. At the same time, the charged links of the both polypeptides began to repel

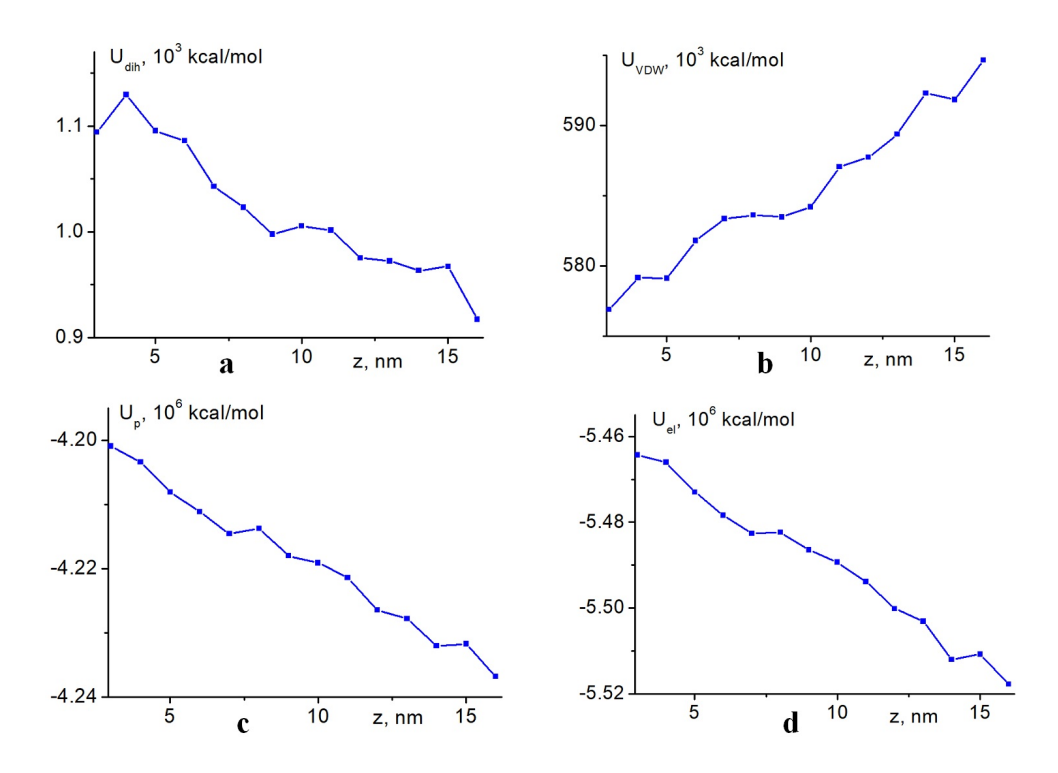


FIG. 7. Dependences of the potential energy of torsion (dihedral) angles (a), van der Waals (b), electrostatic (c) and total potential energy (d) of two polypeptides from glutamic acid units as a function of the average deviation of the centers of mass of the polypeptides from the center of the carbon nanotube along the axis at $pH\approx6-8$

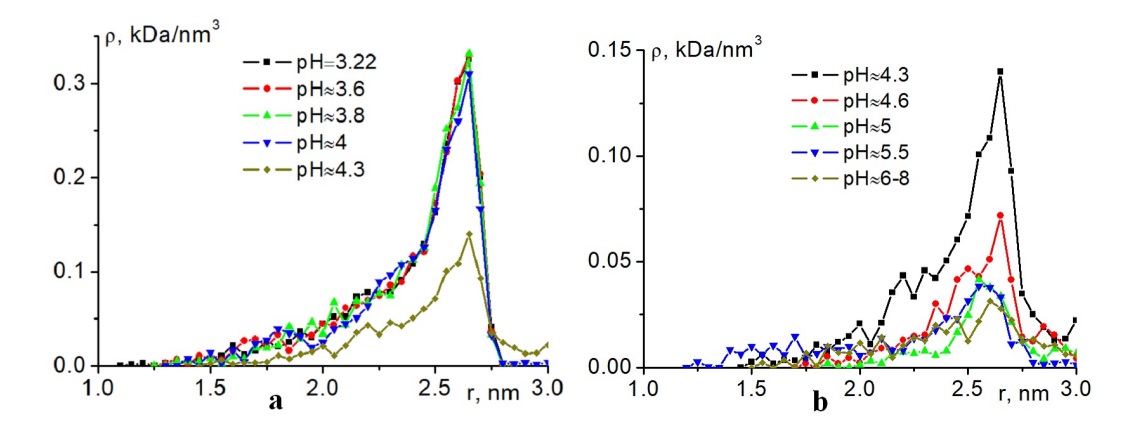


FIG. 8. Total radial dependences of the average density of atoms of two polyglutamate macromolecules inside a carbon nanotube at different values of pH: a) from 3.22 to 4.3, b) from 4.3 to 6–8

each other more and more strongly, which led to the macromolecules shifting outward to the two opposite ends of the nanotube (Fig. 6).

Figure 6a shows that even with a small charge of the macrochain and a small deviation from the isoelectric point $(pH\approx4)$, the polyglutamate molecules begin to shift away from each other. And when half of all the polypeptide links became negatively charged $(pH\approx4.3)$, both charged macromolecules shifted to opposite ends of the carbon nanotube (Figs. 6b,c). A further increase in the pH did not lead to desorption of the polypeptides, but an increasing unfolding of the macrochains was observed due to an increase in their rigidity with the ends of the polypeptides being thrown out into the surrounding space. At the same time, the macrochain remained at the ends of the carbon nanotube, partially wrapping around them (Figs. 6d-f).

Figure 7 shows the dependences of the potential energy of two polyglutamate molecules inside a carbon nanotube on the average deviation of the centers of mass of the polypeptides from the center of the nanotube along the axis at a hydrogen index of pH \approx 6–8. The z axis shows the average absolute value of the distance of the centers of mass of the polypeptides from the center of the nanotube: at z=15 nm, the polypeptides are at the opposite edges of the nanotube (Fig. 6e,f). It is evident that the potential energy of the torsion angles, as in the case of a single macrochain, gradually

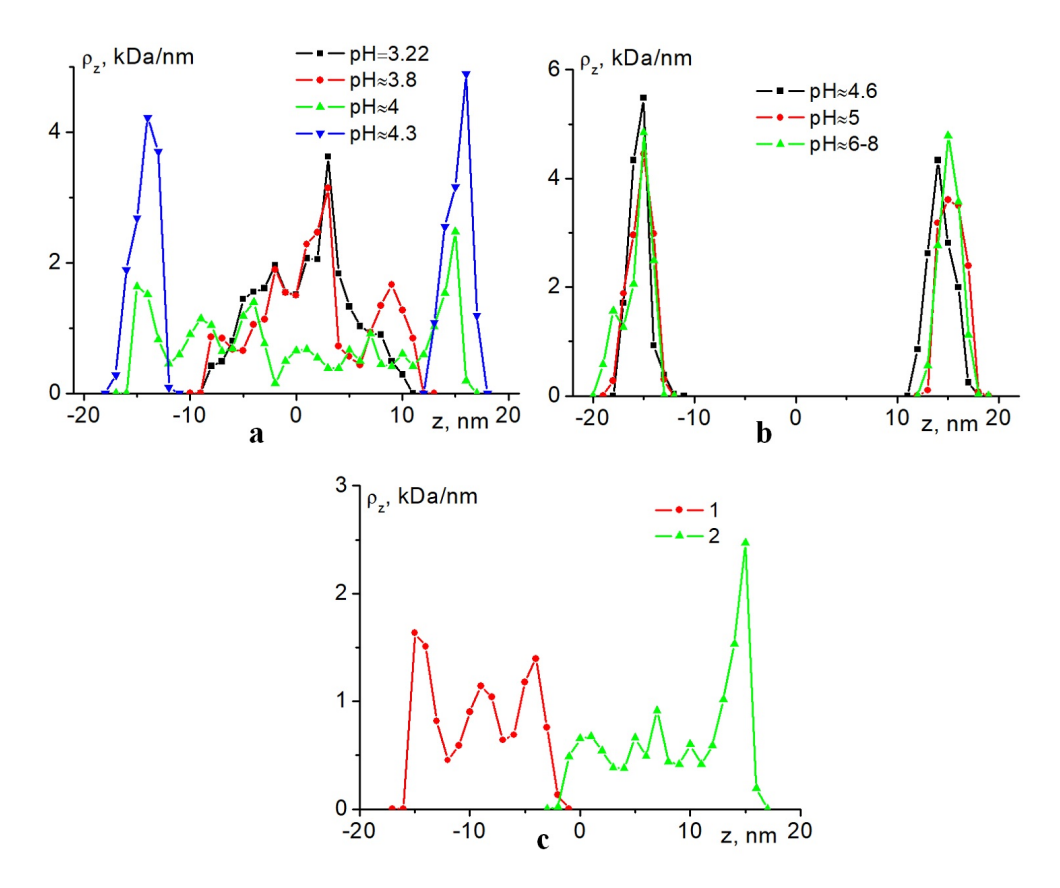


FIG. 9. Total distributions of the average linear density of atoms of two polyglutamate macromolecules along the axis of a carbon nanotube at different values of pH: a) from 3.22 to 4.3, b) from 4.6 to 6–8. c) Distributions of the linear density of atoms of two polyglutamate macromolecules separately (1 and 2) at pH \approx 4

decreased as the polypeptides unfolded and decapsulated from the nanotube (Fig. 7a). At the same time, the potential energy of van der Waals interactions increased (Fig. 7b). The electrostatic energy of the nanosystem decreased much more strongly when the polypeptides were shifted to the edges of the nanotube (Fig. 7c), as in the case of a single polypeptide molecule inside a carbon nanotube. Therefore, the total potential energy of the nanosystem consisting of two charged polypeptides inside a carbon nanotube also decreased upon their decapsulation (Fig. 7d). Thus, as in the case of a single polyelectrolyte, the most energetically favorable conformations were those in which the charged polypeptides were located outside at the ends of the carbon nanotube.

Figure 8 shows the total radial dependences of the average atomic density of two polypeptides from glutamic acid units inside a carbon nanotube at different pH values. It is evident that while both macromolecules are inside the carbon nanotube, i.e. at pH values from 3.22 to 4, the curves of the total radial distributions of their atomic density are very close to each other (Fig. 8a). The radial distribution peaks for the atomic density of the macrochains decreased as the polypeptides moved outward from the nanotube. (Fig. 8b). At the same time, the radial distributions of the average density of each of the polypeptides separately at all pH values were similar to each other.

Figure 9 shows the distributions of the average linear density of atoms of two polyglutamate macromolecules at different pH values along the carbon nanotube axis. At pH<4, the atoms of both macrochains are concentrated in the central part of the nanotube (Fig. 9a). At pH ≈4 , the profile of the total linear distribution of the density of polypeptide atoms spreads out along the entire length of the carbon nanotube (Fig. 9a), while the profiles of the linear density of atoms for individual polypeptides (Fig. 9c) hardly intersect. The case of the location of polypeptides at different ends of the carbon nanotube (pH ≈4.3) corresponds to separate profiles of the linear distributions of the density of atoms with peaks at the ends of the nanotube: about -15 nm and +15 nm along the z axis (Figs. 9a,b).

4. Conclusion

When the pH value deviated from the isoelectric point, the single polypeptide macrochain adsorbed inside the carbon nanotube unfolded more and more and stretched along the nanotube. When all or almost all the polypeptide links became charged, the polypeptide was decapsulated from the carbon nanotube. Thus, by changing the charge of the links and, thereby, the rigidity of the macrochain, it is possible to control the release of the polypeptide molecule encapsulated [20, 21] inside the carbon nanotube. When two identical homogeneous polypeptides were located on the inner surface of the

carbon nanotube, then in case when the pH level deviated from the isoelectric point, they shifted outward to two opposite ends of the nanotube. In this situation, the release of charged macromolecules from the carbon nanotube began to occur when half of the amino acid residues of the polypeptide acquired an electric charge, that is, with a significantly smaller deviation of the pH value from the isoelectric point compared to a single polypeptide. Obviously, further increase in the number of polypeptides inside the carbon nanotube leads to even stronger repulsion of macromolecules from each other when the pH level deviates from the isoelectric point. This can cause not only the exit of polypeptides from the central part of the carbon nanotube to its ends, but also the desorption of macromolecules.

It should be noted that the ends of the carbon nanotube can be oxidized by carboxyl or hydroxyl groups, the presence of which can worsen both the capillary absorption of the polypeptide and complicate the release of the polypeptide from the carbon nanotube. The role of foreign ions was also not taken into account in this study.

If the encapsulated polypeptide contains small medicinal or photoactive molecules in the structure of its macrochain at the isoelectric point, then upon decapsulation of the polypeptide from the carbon nanotube, they can be released from the carbon nanotube or will be concentrated together with the macromolecule near its ends.

Thus, a nanosystem with one or more polypeptides inside a carbon nanotube can be used as a nanocontainer sensitive to changes in the pH of the medium. Encapsulation [20, 21] of polypeptides in a nanotube will be carried out at the isoelectric point, and decapsulation of macrochains will occur at a pH value significantly different from the isoelectric point characteristic of a certain composition of amino acid residues of the polypeptide. Instead of a homogeneous polypeptide, any polypeptide with amino acid residues of different types can be used. Since polypeptides with different sets of links have their own isoelectric point value, then by changing the combination of amino acid residues in the polypeptide, it is possible to select a pH value corresponding to an acidic, alkaline or neutral medium, at which the substances contained therein will be released from the carbon nanotube.

In addition, such a nanosystem can be used as a sensor element sensitive to changes in the hydrogen index of the medium. For example, in a luminescent-optical meter of the concentration of molecular (including singlet) oxygen, the operation of which is sensitive to changes in the conformational structure of a macromolecular chain in a nanopore or nanotube, with photoactive molecules (dyes) contained in the structure of the macromolecule [39]. The non-uniform distribution of photoactive centers associated with the macrochain inside a carbon nanotube has a significant effect on the kinetics of two-stage photoreactions involving electronically excited dye molecules and oxygen, and the shape of the pulse signal of delayed fluorescence depends on this [39]. Therefore, a significant change in the conformational structure of polypeptides together with dye molecules inside a carbon nanotube or nanopore will lead to a change in the shape of the time dependence of the intensity of delayed fluorescence, which will make it possible to create a molecular oxygen sensor sensitive to changes in the pH of the environment.

References

- [1] Balasubramanian K., Burghard M. Biosensors based on carbon nanotubes. Anal Bioanal Chem, 2006, 385, P. 452-468.
- [2] Qi H., M\u00e4der E., Liu J. Unique water sensors based on carbon nanotube-cellulose composites. Sensors and Actuators B: Chemical, 2013, 185, P. 225-230.
- [3] Tilmaciu C-M., Morris M.C. Carbon nanotube biosensors. Front. Chem., 2015, 3, P. 59.
- [4] Ferrier D.C., Honeychurch K.C. Carbon nanotube (CNT)-based biosensors. *Biosensors*, 2021, 11, P. 486.
- [5] Ranjbari S., Bolourinezhad M., Kesharwani P., Rezayi M, Sahebkar A. Applications of carbon nanotube biosensors: Sensing the future. *Journal of Drug Delivery Science and Technology*, 2024, **97**, P. 105747.
- [6] Dewey H.M., Lamb A., Budhathoki-Uprety J. Recent advances on applications of single-walled carbon nanotubes as cutting-edge optical nanosensors for biosensing technologies. *Nanoscale*, 2024, **16**, P. 16344–16375.
- [7] Gazzato L., Frasconi M. Carbon nanotubes and their composites for flexible electrochemical biosensors. *Analysis & Sensing*, 2025, 5, P. e202400038.
- [8] Bianco A., Kostarelos K., Prato M. Applications of carbon nanotubes in drug delivery. *Current Opinion in Chemical Biology*, 2005, **9**(6), P. 674–679.
- [9] Meng X., Zhang Z., Li L. Micro/nano needles for advanced drug delivery. Progress in Natural Science: Materials International, 2020, 30(5), P. 589–596.
- [10] Alshawwa S.Z., Kassem A.A., Farid R.M., Mostafa S.K., Labib G.S. Nanocarrier drug delivery systems: characterization, limitations, future perspectives and implementation of artificial intelligence. *Pharmaceutics*, 2022, **14**, P. 883.
- [11] Roxbury D., Zhang S., Mittal J., DeGrado W.F., Jagota A. Structural stability and binding strength of a designed peptide-carbon nanotube hybrid. *J. Phys. Chem. C*, 2013, **117**, P. 26255–26261.
- [12] Wang H., Michielssens S., Moors S.L.C., Ceulemans A. Molecular dynamics study of dipalmitoylphosphatidylcholine lipid layer self-assembly onto a single-walled carbon nanotube. Nano Res., 2009. 2, P. 945–954.
- [13] Roxbury D., Manohar S., Jagota A. Molecular simulation of DNA β -sheet and β -barrel structures on graphite and carbon nanotubes. *J. Phys. Chem. C*, 2010, **114**, P. 13267–13276.
- [14] Li L., Cao Q., Liu H., Qiao X., Gu Z., Yu Y., Zuo C. Understanding interactions between poly(styrene-cosodium styrene sulfonate) and single-walled carbon nanotubes. *J Polym Sci.*, 2021, **59**, P. 182–190.
- [15] Kruchinin N.Yu., Kucherenko M.G. Molecular dynamics simulation of the conformational structure of uniform polypeptides on the surface of a polarized metal prolate nanospheroid with varying pH. Russian Journal of Physical Chemistry A, 2022, 96(3), P. 624–632.
- [16] Kruchinin N.Yu. Molecular dynamics simulation of the rearrangement of polyampholyte conformations on the surface of a charged oblate metal nanospheroid in a microwave electric field. *Nanosystems: Physics, Chemistry, Mathematics*, 2023, **14**(6), P. 719–728.
- [17] Kruchinin N.Yu., Kucherenko M.G. Conformational structure of a complex of two oppositely charged polyelectrolytes on the surface of a charged spherical metal nanoparticle. *High Energy Chemistry*, 2024, **58**(6), P. 615–623.

- [18] Kruchinin N.Yu., Kucherenko M.G. Conformational changes of two oppositely charged polyelectrolytes, including those combined into a single block copolymer, on the surface of a charged or transversely polarized cylindrical metal nanowire. *Journal of Polymer Research*, 2025, **32**(3), P. 79.
- [19] Salimi A., Compton R.G., Hallaj R. Glucose biosensor prepared by glucose oxidase encapsulated sol-gel and carbon-nanotube-modified basal plane pyrolytic graphite electrode. *Anal Biochem*, 2004, **333**(1), P. 49–56.
- [20] Chen Q., Wang Q., Liu Y.-C., Wu T., Kang Y., Moore J.D. Gubbins K. E. Energetics investigation on encapsulation of protein/peptide drugs in carbon nanotubes. *The Journal of Chemical Physics*, 2009, **131**(1), P. 015101.
- [21] Kang Y., Wang Q., Liu Y.-C., Wu T., Chen Q., Guan W.-J. Dynamic mechanism of collagen-like peptide encapsulated into carbon nanotubes. *The Journal of Physical Chemistry B*, 2008, **112**(15), P. 4801–4807.
- [22] Kang Y., Liu Y.-C., Wang Q., Shen J.-W., Wu T., Guan, W.-J. On the spontaneous encapsulation of proteins in carbon nanotubes. Biomaterials, 2009, 30(14), P. 2807–2815.
- [23] Zhang Z., Kang Y., Liang L., Liu Y., Wu T., Wang Q. Peptide encapsulation regulated by the geometry of carbon nanotubes. Biomaterials, 2014, 35(5). P. 1771–1778.
- [24] Yang N., Chen X., Ren T., Zhang P., Yang D. Carbon nanotube based biosensors. Sensors and Actuators B: Chemical, 2015, 207(A), P. 90–715.
- [25] Chavan K.S., Barton S.C. Confinement and Diffusion of Small Molecules in a Molecular-Scale Tunnel. *Journal of The Electrochemical Society*, 167, P. 023505.
- [26] Li W., Cheng S., Wang B., Mao Z., Zhang J., Zhang Y., Liu Q.H. The transport of a charged peptide through carbon nanotubes under an external electric field: a molecular dynamics simulation. RSC Adv., 2021, 11, P. 23589–23596.
- [27] Chen Q., Liang L., Zhang Z., Wang Q. Release of an encapsulated peptide from carbon nanotubes driven by electric fields: a molecular dynamics study. ACS Omega, 2021, 6(41), P. 27485–27490.
- [28] Andrade L.R.M., Andrade L.N., Bahú J.O., Concha V.O.C., Machado A.T., Pires D.S., Santos R., Cardoso T.F.M., Cardoso J.C., Albuquerque-Junior R.L.C., Severino P., Souto E.B. Biomedical applications of carbon nanotubes: A systematic review of data and clinical trials. *Journal of Drug Delivery Science and Technology*, 2024, 99, P. 105932.
- [29] Batys P., Morga M., Bonarek P., Sammalkorpi M. pH-Induced Changes in Polypeptide Conformation: Force-Field Comparison with Experimental Validation. J. Phys. Chem. B, 2020, 124(14), P. 2961–2972.
- [30] Resende L.F.T., Basilio F.C., Filho P.A., Therézio E.M., Silva R.A., Oliveira O.N., Marletta A., Campana P.T. Revisiting the conformational transition model for the pH dependence of BSA structure using photoluminescence, circular dichroism, and ellipsometric Raman spectroscopy. *International Journal of Biological Macromolecules*, 2024, **259**(1), P. 129142.
- [31] Stepanenko D., Wang Y., Simmerling C. Assessing pH-Dependent Conformational Changes in the Fusion Peptide Proximal Region of the SARS-CoV-2 Spike Glycoprotein. Viruses, 2024, 16, P. 1066.
- [32] Phillips J.C., Braun R., Wang W., Gumbart J., Tajkhorshid E., Villa E., Chipot C., Skeel R.D., Kalé L., Schulten K. Scalable molecular dynamics with NAMD. J Comput Chem., 2005, 26, P. 1781–1802.
- [33] MacKerell Jr. A.D., Bashford D., Bellott M., Dunbrack Jr. R.L., Evanseck J.D., Field M.J., Fischer S., Gao J., Guo H., Ha S., Joseph-McCarthy D., Kuchnir L., Kuczera K., Lau F.T.K., Mattos C., Michnick S., Ngo T., Nguyen D.T., Prodhom B., Reiher W.E., Roux B., Schlenkrich M., Smith J.C., Stote R., Straub J., Watanabe M., Wiórkiewicz-Kuczera J., Yin D., Karplus M. All-atom empirical potential for molecular modeling and dynamics studies of proteins. *J. Phys. Chem. B.*, 1998, **102**(18), P. 3586–3616.
- [34] Huang J., Rauscher S., Nawrocki G., Ran T., Feig M., de Groot B.L., Grubmüller H., MacKerell Jr. A.D. CHARMM36m: an improved force field for folded and intrinsically dis-ordered proteins. Nature Methods, 2016, 14, P. 71–73.
- [35] Radak B.K., Chipot C., Suh D., Jo S., Jiang W., Phillips J.C., Schulten K., Roux B. Constant-pH Molecular Dynamics Simulations for Large Biomolecular Systems. J. Chem. Theory Comput., 2017, 13(12), P. 5933–5944.
- [36] Zhu F, Schulten K. Water and Proton Conduction through Carbon Nanotubes as Models for Biological Channels. *Biophysical Journal*, 2003, 85(1), P. 236–244.
- [37] Darden T., York D., Pedersen L. Particle mesh Ewald: An N·log(N) method for Ewald sums in large systems. J. Chem. Phys., 1993, 98, P. 10089– 10092
- [38] Jorgensen W.L., Chandrasekhar J., Madura J.D., Impey R.W., Klein M.L. Comparison of simple potential functions for simulating liquid water. J. Chem. Phys., 1983, 79, P. 926–935.
- [39] Kucherenko M.G., Rusinov A.P., Chmereva T.M., Ignat'ev A.A., Kislov D.A., Kruchinin N.Yu. Kinetics of photoreactions in a regular porous nanostructure with cylindrical cells filled with activator-containing macromolecules. *Optics and Spectroscopy*, 2009, 107(3), P. 480–485.

Submitted 20 March 2025; revised 17 September 2025; accepted 06 October 2025

Information about the authors:

Nikita Yu. Kruchinin – Orenburg State University, Center of Laser and Informational Biophysics, Orenburg, Russia; OR-CID 0000-0002-7960-3482; kruchinin_56@mail.ru

Conflict of interest: the authors declare no conflict of interest.